Light Metals 2014
Edited by: John Grandfield
TMS (The Minerals, Metals & Materials Society), 2014

SIMULATION OF ANODE BUBBLE: VOLUME OF FLUID METHOD

Yiwen Zhou [1, 2], Jiemin Zhou [1], Jianhong Yang [2], Wangxing Li [2], Shouhui Chen[2]
[1] School of Energy Science and Engineering, Central South University; Lushan Road; Changsha, Hunan, 410083, China
[2] Zhengzhou Reseach Institute of Chalco; Jiyuan Road 82#,Shangjie District; Zhengzhou,Henan, 450041,China

Keywords: Simulation; Bubble; Volume of Fluid; Flow Pattern

Abstract

In an aluminum reduction cell, bubbles are generated on the anode surfaces. Before they get out of the bath, they linger over between gap of the anode and the cathode, which leads to additional voltage drop. The alumina concentration adjacent to the anode is also affected. How are the bubbles formed and what kinds of shape they have are the important issues. Numerical simulation can provide detailed information about bubbles. The volume of fluid model (VOF) was applied in the bubble simulation. The flow difference between different locations was presented.

Introduction

In an aluminum reduction cell, the direct current comes from the cathode collector bar of upstream cell through the bus bar system to the anode rod. The electrical current then passes from the carbon anodes via the molten bath, containing alumina in solution, to the carbon cathode cell lining. As the electrical current passes through the solution, the aluminum oxide is decomposed into molten aluminum (Al) and oxygen (O_2). The oxygen consumes the carbon (C) in the anode blocks to form carbon dioxide (CO_2), which is released. The primary cell reaction is given by[1]

$$2Al_2O_3(\text{dissolved}) + 3C(solid) \rightarrow Al(liquid) + 3CO_2(gas) \quad (1)$$

During operation, the anodes are continually lowered to maintain a constant anode cathode distance (ACD), and eventually replaced. The carbon dioxide gas produced on the underside of each anode forms bubbles that move away toward the edges of the anode. When bubbles come into contact with each other, they can coalesce. This bubble layer underneath the approximately horizontal anode surface is about 5.3-12.5 mm thick[2]. When the bubbles detaches from the anode, they rise rapidly because of their buoyancy and escaped up the side of the anode. The rate of gas evolution at the underside of the anode is fairly high. Motivated by the gas bubble, the movements of the bath forms the flow patterns. Ideally, the bath keeps alumina concentration at a uniform level throughout the bath volume with as little variation as possible. Practically, the alumina concentration varies from place to place in the industrial cell. Moreover, owing to the non-conductivity of the bubble, the extra ohmic drop in the electrolyte due to the presence of gas bubbles may be in the range of 0.15-0.35V[3]. Consequently, the flow pattern induced by bubbles is the important issue. The objective of the present investigation is to determine an appropriate model for predicting the flow pattern.

Method about Bubble Investigation

Different kinds of methods are introduced in investigation of bubble behavior according to the bubble generation mechanism. The first approach used is the direct study in the real aluminum reduction cells. The severe operation environment of high temperature, corrosiveness of bath and difficulty of access makes the measurements almost impossible. Data about gas obtained from real cell were few and far between. Kobbeltvedt[4] measured the gas released from the real cell with a funnel. The measurement showed clearly that the gas release into the center channel was dependent upon location. The gas released from the anode with high bath flow was uneven in side channel and center channel. While the gas released from the anode with low bath flow was almost the same in side channel as it was in center channel.

The second approach used is simulated by electrolysis experiments carried out in laboratory with the same anode, cathode and electrolyte but in different dimensions. The electrolysis process was observed by quartz see-through cell and radiography techniques [5-7]. The experiments were carried out in a graphite crucible in a gas-tight vertical quartz tube. Images of the cell were formed on a photographic film by a horizontal beam of X-rays. During the growth of a single bubble under the anode base, the electrolyte was pushed away from the surface. The gas formation started with a whole series of small bubbles under the anode. These bubbles would gradually grow together and form a thin continuous gas film. The thickness of the gas film would gradually grow and contact angles ranges from 30 up to 160 degree were observed.

The third approach used is simulated by low temperature of electrolysis of similar electrochemical reaction. The analogous experiment[8, 9] with environmental temperature was designed using copper sulfate liquor as electrolyte，a piece of carbon as anode to simulate the process of anodic bubble's growth，merging and movement，and the rules of bubble size and movement were carried out． The change of inclination of anode has significant influence to the bubble's velocity and merging.

The fourth approach used is physical simulation by water and pressed air. S. Fortin [10] constructed a full-scale mode of a two dimensional transverse section through a 150kA prebake aluminum reduction cell. Gas evolution on the anode face was simulated by passing air through polyethylene plate. The observed result indicated that the anode cathode distance had no effect on gas bubble behaviour. An increase in current density increased the bubble size and thickness of bubble front as well as gas coverage of the anode face and bubble velocity. Behavior of the gas layer on horizontal anode was different than on a inclined anode. On a horizontal anode, the process of bubble nucleation, growth, coalescence and release involved no bubble motion and led to a gas layer thickness of approximately 5 mm.By passing compressed gas through the a Plexiglas plate immersed in water, Xiangpeng Li[11] investigated the gas evolution, bubble behavior and liquid flow field. T. Utigard [5-7] observed that when

external gas was bubbled into the electrolyte through a vertical hole located in the center of the anode, there was no significant difference in behavior between different gases used and the bubble grew in size in a manner similar to that observed when electrolysis was performed.

The fifth approach used is simulated by numerical simulation. Numerical modeling provides the opportunity to determine flows, gas formation, etc in great detail without risk. Plenty of articles were published by using the numerical simulation of the aluminum reduction cell on thermal, electrical, magnetic or fluid dynamical issues. In Buffo's[12] work Conditional Quadrature Method (CQMOM) of Moments and Direct Simulation Monte Carlo predictions are compared and results show that CQMOM is an accurate tool for the simulation of bivariate PBE for gas-liquid systems. Feng[13] modeled the bubble induced turbulence by modifying bubble induced turbulence viscosity directly and by modifying bubble induced turbulence kinetic energy in a standard k-ε turbulence model. Both models can capture the key flow patterns which are comparable with PIV measurement, while the modified turbulence kinetic energy model gives better agreement with flow patterns in the anode cathode distance (ACD). Caboussat [14] numerically investigated the large bubbles rising under an inclined plane by volume-of-fluid method. Numerical simulations are in excellent agreement with experimental data. Among models for gas-liquid system, the VOF model could interpret both the bubble shape and flow pattern. Therefore, the VOF model is used in the present work.

Lagrangian or Eulerian

The flow about bubble movement in the electrolyte is a two-phase flow. For the modeling of two-phase flows one may choose to treat both the dispersed and continuous phase as interpenetrating pseudo-continua as in the Euler-Euler approach or the dispersed phase as discrete entities as in the Euler-Lagrange approach. The Euler-Lagrange approach[15], also known as the discrete phase model, is best used for flow regimes where the difference between the volume fractions of the two phases is large. The discrete phase model injects a large number of particles into the primary phase and then uses a force-balance equation in the Lagrangian reference frame to calculate the effect that the primary phase has upon the trajectory of each particle. Typically, the secondary phase should not make up more than 10% of the total volumetric flowrate. Two-phase simulations at higher hold-up have problems with convergence together with an increased computational load. Therefore, the Euler-Lagrange approach was mainly applied to determine dispersion coefficients from a small amount of droplets. The Eulerian model is appropriate to cases where the volume fraction of the dispersed phase is high and varies widely, which is actually the situation in an aluminum reduction cell. Over the last years the Euler-Euler approach emerged as the standard approach to model multiphase problems at higher hold-up. In the Euler-Euler approach[16], the different phases are treated mathematically as interpenetrating continua. Since the volume of a phase cannot be occupied by the other phases, the concept of phase volume fraction is introduced. These volume fractions are assumed to be continuous functions of space and time and their sum is equal to one.

Since the number of bubble is great and the bubble accumulates under the anode bottom surface in an aluminum reduction cell, the using of Euler-Lagrange approach will lead to convergence problem and very expensive of computational cost. The Euler-Euler approach is the better option for the simulation of flow pattern induced by bubble. Consequently, the Euler-Euler approach is adopted in this investigation.

Model Description

The simulation completed in the commercial software CFX. The degassing boundary condition was set at the top of the bath to allow air escaping. The faces formed by active points were set as wall with a boundary source where the air was introduced into the cell. The symmetry condition was set at center channel. The other boundaries were set as walls (no slip for water and free slip for air). The homogeneous free surface model in CFX was used to simulate the bubble behavior.

In order to compare with experiment observation results in physical simulations, the numerical model uses the same water *'cell'*. As shown in Table 1, in the model, water was used as bath and air as CO_2 produced in the aluminum reduction cell.

Table 1 Comparison between water model and industrial cell

	Water model	*Industrial cell[17]*
Bath	water	Fluoride melt
Metal	no	Aluminum
Gas	air	CO_2
Operation temperature(℃)	Room temperature	~950
Kinematic viscosity of bath ($m^2 \cdot s^{-1}$) •	1.5E-6	~1.5E-6
Kinematic surface tension ($m^3 \cdot s^{-2}$)	7.3E-5	~6.3E-5
Anode dimensions (mm)	412.5*165	1650*660
Anode-cathode-distance(mm)	40	40
Bath Height (mm)	200(water)	200

Limited by the computer resources, a quarter of one anode was included in the model. And the distance between the anode and side wall and the distance of the middle gap was also reduced to a quarter of those. The CO_2 is produced at the active points of the anode bottom in the real aluminum reduction ell. In this mode, a square face of 5mm×5mm stands as this kind of active point. There are matrix of 15 rows and 39 columns of active points distributed on the anode bottom as the gas inlet in this mode as shown in Figure 1. In order to obtain the detail of bubble behavior, denser grids were set in the regions under and adjacent to the anode as shown in Figure 2. Altogether, there are 1,676,325 elements in the model. It takes 11days and 10 hours to have the 1000s of transient model solved on a Dell PowerEdge Server R900 with 8 CPU cores.

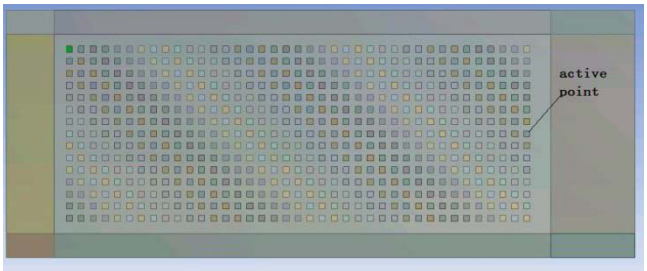

Fig.1 Active points under the anode

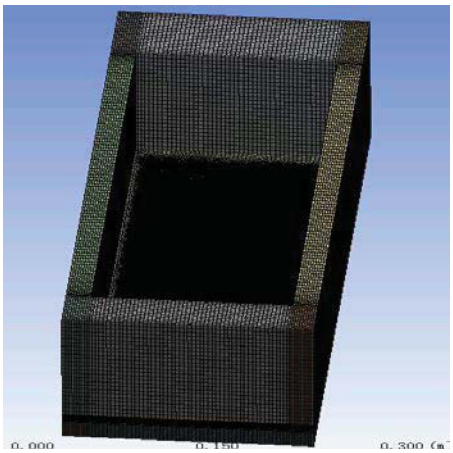

Fig.2 FEA meshing model

Results and Discussion

Three vertical planes (LA, LB, LC) paralleled to the anode length direction and five planes (WA, WB, WC, WD, WE) paralleled to the anode width direction and a horizontal plane in the middle of the ACD were selected to describe the key flow structures.

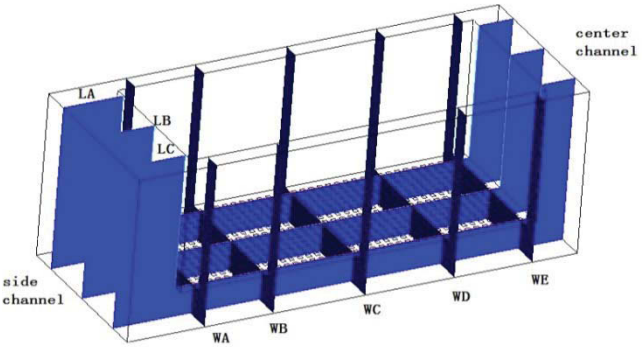

Fig. 3 Position of planes

The water velocity distribution at the horizontal plane in middle of ACD is shown in figure4. The result in Figure 5 shows the PIV[13] measurement result of the water velocity distribution of the air-water cold model experiment. Geometrically, the quarter anode in this model is more like the anode at the duct end than the other two anodes in Figure 5. Compared with that in Figure5, the magnitude of water velocity in Figure 4 is of the same order. Both of the water at the side channel and center channel in Figure 4 and 5 move toward the anode with no local circulation. Except the circulation, the streamline at the duct end in Figure 4 appears similar as that of the PIV test in Figure 5. The simulation can predict key flow patterns which are comparable with PIV measurement.

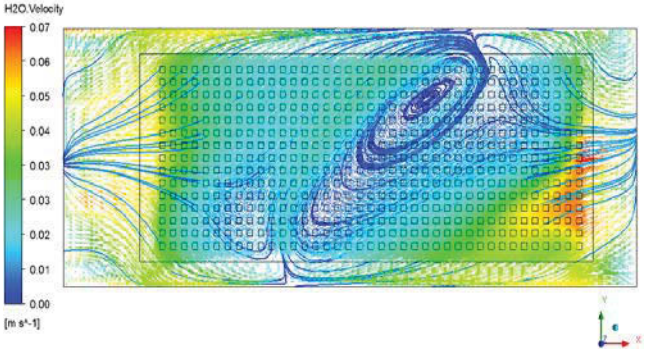

Fig.4 Water velocity distribution at the horizontal plane in middle of ACD- simulation.

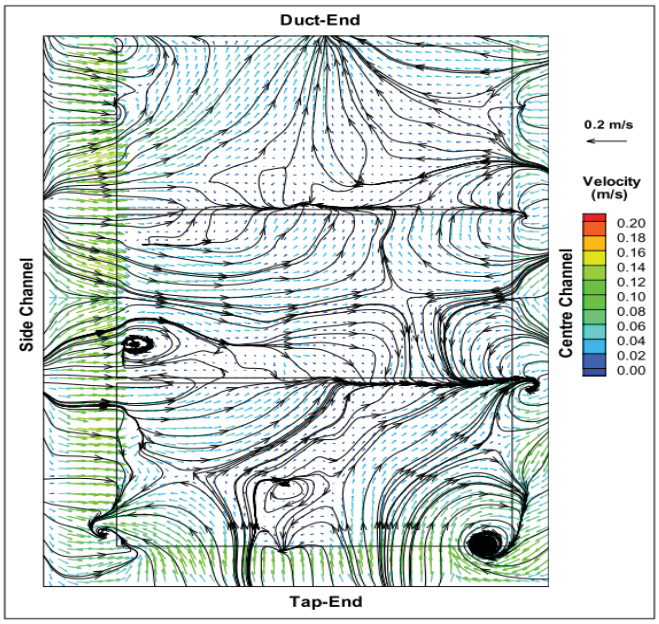

Fig. 5 Water velocity distribution at the horizontal plane in middle of ACD- PIV measurement[13]

As shown in Figure 6 and Figure 7, there is a thin layer of air at the bottom and side of the anode. The volume fractions of air at the anode bottom at different vertical planes are similar. At the anode bottom adjacent to the edge, the volume fraction of air is reduced, which is due to the gas leaving from the anode bottom. At the edge of the anode, the gas leaves the anode bottom right after it is produced. At the anode bottom, the bubbles far from the edge push the bubbles in front of itself forward to the edge. Consequently, the bubbles near the edge accumulate and grow bigger. Then they leave the bottom surface of the anode and are splited into two parts by anode edge. The parts outside of the anode bottom will go upward, and the parts remained under the anode bottom retreat back to maintain the ellipsoid shape due to the surface tension and pressure.

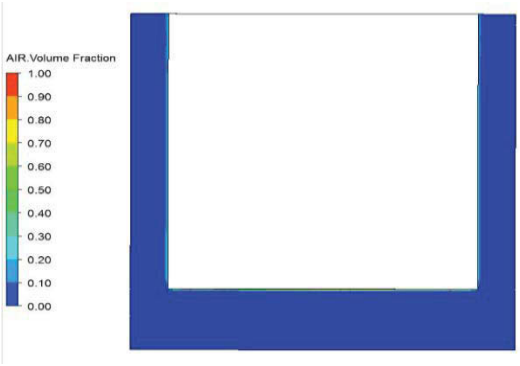

Fig. 6 Volume fraction of air at vertical plane WC

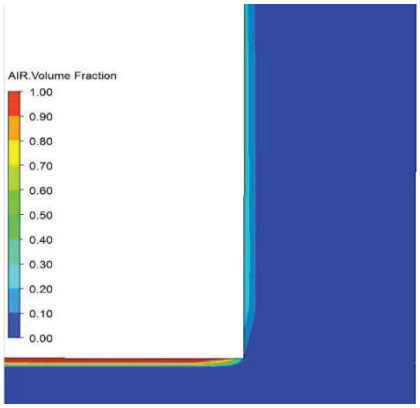

Fig. 7 Volume fraction of air at vertical plane WC at side channel

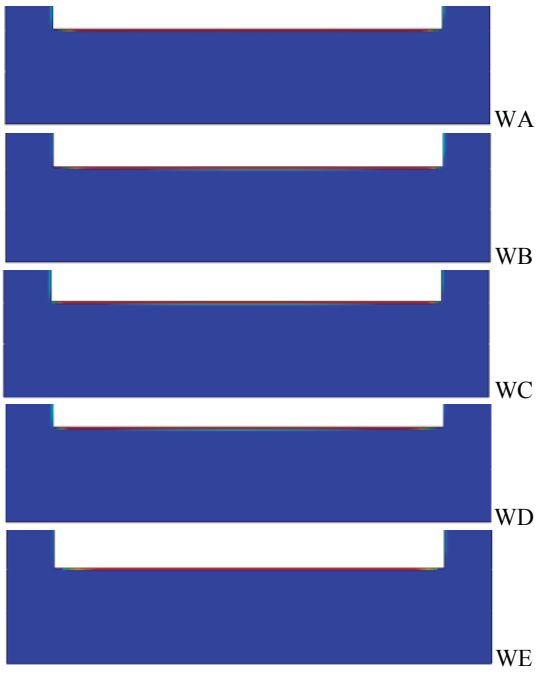

Fig. 8 Volume fraction of air at vertical planes

The result in Figure 8 shows the volume fraction of air varies at different location. Volume fractions of air at the vertical plane of WA and WE are evenly distributed except at the location near the anode edge. And there are zones with high volume fraction of air at two ends of the vertical plane of WB, WC and WD, at where probably the Fortin bubble located.

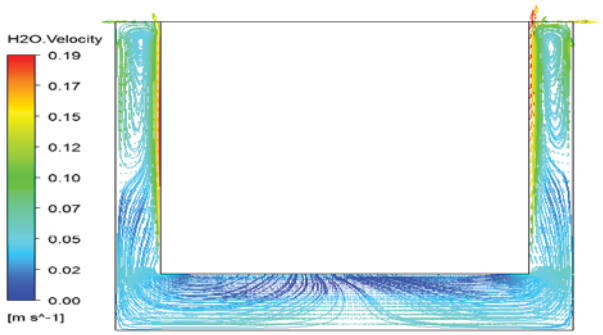

Fig. 9 Water velocity distribution and streamlines at plane WA

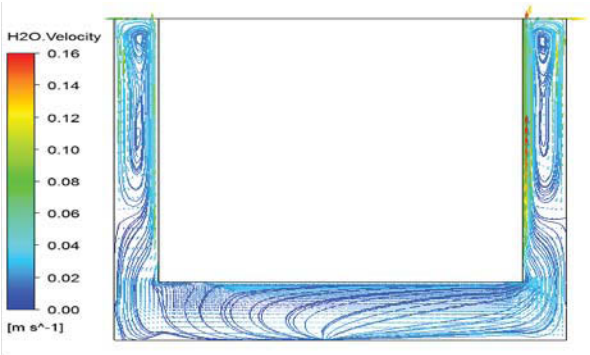

Fig. 10 Water velocity distribution and streamlines at plane WB

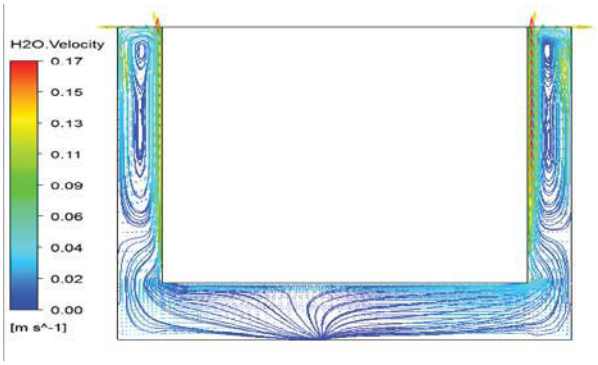

Fig. 11 Water velocity distribution and streamlines at plane WC

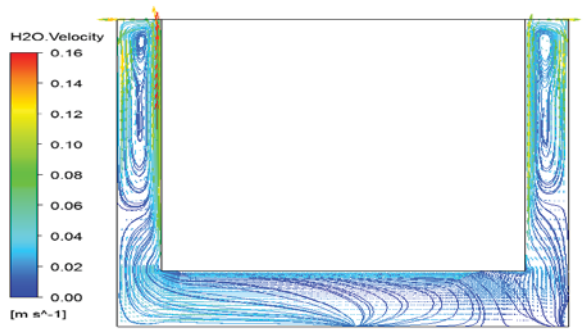

Fig. 12 Water velocity distribution and streamlines at plane WD

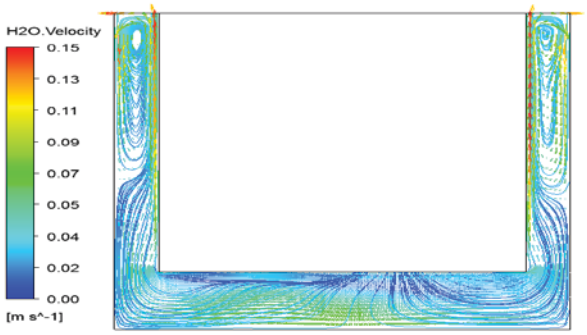

Fig. 13 Water velocity distribution and streamlines at plane WE

Fig. 14 Water velocity distribution and streamlines at plane LA

Fig. 15 Water velocity distribution and streamlines at plane LB

Fig. 16 Water velocity distribution and streamlines at plane LC

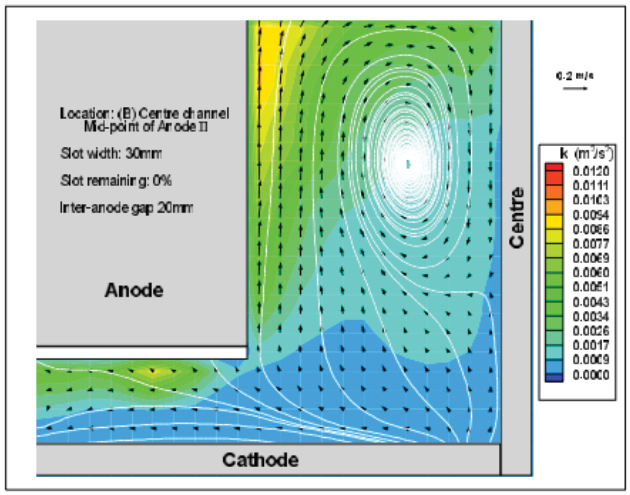

Fig 17. Water velocity distribution and streamlines in center channel at anode II[18]

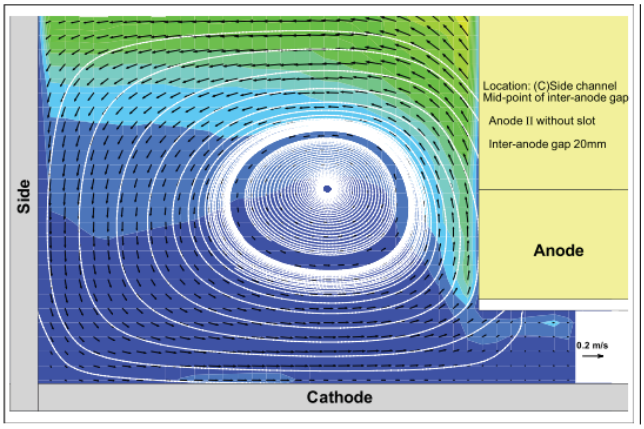

Fig 18. Water velocity distribution and streamlines in side channel at anode II[19]

The results in Figures 9 to 13 show the water flow and streamlines over the vertical planes in the inter-anode channel and the inter-polar zones. One common feature of the flow in these planes is the presence of a local recirculation zone. The bubble released from the anode bottom change direction and rise upward along the anode side at the anode edge due to the buoyancy force. Consequently, water is pushed upward. The water flow change its direction horizontally toward the neighboring walls at the top surface, then it flows downward paralleled to the neighboring walls, completing the recirculation by joining the upward flow under the anode.

The streamlines in plane WA in Figure 9 show that the fluid from the middle of anode bottom surface goes downward and are separated into two streams, one to the left and one to the right. Then the two streams flow along the bottom of the cell till they reach the side boundary where they go upward along with flow under the anode. During the rising process, the flow clings to the anode side surface. After arriving at the top surface, it moves along the top surface and the side boundary and then recirculates at the half height of the anode. The results in Figure 10 to Figure 13 show that the streamlines in the inter-anode channel in plane WB, WC, WD and WE are similar like those in plane WA. The

shapes of recirculation in the inter-anode channel are long and narrow, but the centers of the recirculation are varying from different planes. In the inter-polar zones, the streamlines in plane WA and WE are mirror symmetry, and those in plane WB and WD are likewise the same. But the streamlines under the anode in plane WA, WB and WC are quite different.

The results in Figure 14 to 16 show the water flow and streamlines over the vertical planes in the center channel (left), side channel (right) and the inter-polar zones. Pumped by the rising of bubble, the fluids rise upward at the anode side at the center channel and side channel, and the local recirculation is formed at each channel. Unlike what was observed by Feng [13] that there is no local recirculation at the narrow channel(duct end channel), there is recirculation at every inter-anode channel, center channel and side channel. The result of PIV measurement[18] of flow pattern in the center channel is presented in Figure 17, the corresponding simulation result of the same position is the left part in Figure 15. The result of PIV measurement[19]of flow pattern in the side channel is presented in Figure 18, the corresponding simulation result of the same position is the right part in Figure 15. Both PIV and simulation results show the flow directions related to the anode are the same, and there is recirculation in the center channel. By comparison, the shape of recirculation of simulation is longer and more narrow than that of the PIV measurement, which probably caused by the quartered size of center channel and side channel in simulation.

The flow patterns in inter-anode channels in the same plane are similar, but the flow pattern in the center channel differs to that in the side channel. These observations demonstrate a significant effect of channel width on flow structures, which agreed with investigation results of Feng[13].

The water flow velocity is much stronger in the side and center channels and inter-anode gaps than that beneath the anode. The denser mesh in this simulation results to more streamline under the anode and vivid description of the flow structure. The vortex of streamline under the anode is presented in Figure 15. Using a denser mesh around the anode may lead to capturing more details about bubble behavior.

Conclusions

Using a quarter model of one anode of an aluminum reduction cell, the bubble driven flow models have been developed. The active points of gas release at the anode bottom are simulated by matrix of square sources. The bubble induced flow has been modeled by volume of fraction model. At the anode bottom adjacent to the edge, the volume fraction of air is reduced. There is recirculation at every channel but their centers are varying from different planes. The water flow velocity is much stronger in the side and center channels and inter-anode gaps than beneath the anode.

Acknowledgements

The financial support by Aluminum Corporation of China Limited is appreciated.

References

1. Group, A.a.N.Z.M.i.I.S., *Bubble formation and movement in aluminium reduction cells*. 1988. p. 33-39.
2. Hyde, T.M. and B. J. Welch, *The Gas under Anodes in Aluminium Smelting Cells Part I: Measuring and Modelling Bubble Resistance under Horizontally Oriented Electrodes.* Light Metals, 1997: p. 333-340.
3. Zhuxian, Q., *Aluminum Smelting in Prebaked Anode Cell (In Chinese)*. 2005: Beijing.
4. Kobbeltvedt, O. and B.P. Moxnes, *On the bath flow, alumina distribution and anode gas release in aluminium cells.* TMS Light Metals, 1997: p. 369-376.
5. Cassayre, L., T. Utigard, and S. Bouvet, *Visualizing gas evolution on graphite and oxygen-evolving anodes.* Journal of Metals, 2002. **54**(5): p. 41-45.
6. Utigard, T.A., J.M. Toguri, and S.W. Ip, *Direct observation of the anode effect by radiography.* TMS Light Metals, 1988: p. 703-706.
7. Cassayre, L., et al., *Gas evolution on graphite and oxygen-evolving anodes during aluminium electrloysis.* Light Metals 2006, 2006: p. 379-383.
8. Yuqing, X., Z. Nai-jun, and B. Sheng-zhong, *Normal temperature analogue experiment of anode bubble's behavior in aluminum electrolysis cells.* The Chinese Journal of Nonferrous Metals, 2006. **16**(10): p. 1823-1828.
9. Alam, M., et al., *Investigation of Electrolytic Bubble Behaviour in Aluminium Smelting Cell.* Light Metals, 2013: p. 591-596.
10. Fortin, S., M. Gerhardt, and A.J. Gesing, *Physical Modelling of Bubble Behaviour and Gas Release from Aluminum Reduction Cell Anodes*, in *Light Metals*. 1984. p. 721-741.
11. Xiangpeng, L., et al., *Physical modeling of gas induced bath flow in drained aluminum reduction cell.* Trans. Nonferrous Met. Soc. China, 2004. **14**(5): p. 1017-1022.
12. Buffo, A., et al., *Simulation of coalescence ,break up and mass transfer in gas-liquid systems by uing Monte Carlo and quarature-based moment methods.* Ninth International Conference on CFD in the Minerals and Process Industries, 2012.
13. Feng, Y.Q., et al., *Development of bubble driven flow CFD model applied for aluminium smelting cells.* Seventh International Conference on CFD in the Minerals and Process Industries 2009: p. 220-227.
14. Caboussat, A. and J. Rappaz, *Numerical Simulation of Bubbles under an Inclined Plane: Application to Aluminum electrolysis.* EPFL-MATHICSE Report, 2010.
15. Shams, E., J. Finn, and S.V. Apte, *A numerical scheme for Euler-Lagrange simulation of bubbly flows in complex systems.* International Journal for Numerical Methods in Fluids, 2010. **67**(12).
16. Kozic, et al. *Comparison of Euler-Euler and Euler-Lagrange Approach in Numerical Simulation of Multiphase Flow in Ventilation Mill-air Mixing Duct*. in *Trid Serbian(28th YU) Congress on Theoretical and Applied Mechanics*. 2011. Vlasina lake, Serbia
17. Solheim, A., J.S. T, and R. S., *Gas driven flow in Hall-Heroult cells.* Light Metals, 1989: p. 245-252.
18. Cooksey, M.A. and W.W. Yang, *Effect of slot height and width on liquid flow in physical models of aluminium reduction cells.* Light Metals 2007 TMS, 2007: p. 451-456.
19. Cooksey, M.A. and W. Yang, *PIV Measurement of Physical Models of Aluminium reduction cells.* Light Metals. 2006 TMS, 2006: p. 359-365